# Mechanism of sign inversion of spontaneous polarization in ferroelectric Sm*C** liquid crystals

Yoshitaka Mieda,[1,*] Hajime Hoshi,[1] Yoichi Takanishi,[1] Hideo Takezoe,[1] and Boštjan Žekš[2]
[1]*Department of Organic and Polymeric Materials, Graduate School of Science and Engineering, Tokyo Institute of Technology, O-okayama, Meguro-ku, Tokyo 152-8552, Japan*
[2]*Institute of Biophysics, Medical Faculty, Lipičeva 2, 1105 Ljubljana, Slovenia*
(Received 5 October 2002; published 13 February 2003)

The ferroelectric liquid crystal FLC-117, which is known to exhibit at a certain temperature the sign inversion of spontaneous polarization $P_s$, is studied under an electric field. From the analysis of the electro-optic response and the direct texture observations, it is concluded that the inversion temperature of $P_s$ has the applied voltage dependence. To interpret our experimental result, we introduce a coupling term between the molecular dipole moments and the magnitude of the applied electric fields to the asymmetric rotational potential about the molecular long axis. The simulated results using this potential are in accordance with our experimental result.

DOI: 10.1103/PhysRevE.67.021701 PACS number(s): 61.30.−v, 77.80.−e

## I. INTRODUCTION

The local ferroelectricity that characterizes the chiral smectic-*C* (Sm*C**) liquid crystal is due to the cooperative hindered rotation about the molecular long axis of the constituent molecules. In 1973, McMillan proposed a simple physical picture of the smectic-*C* (Sm*C*) phase; the molecules rotate freely about their long axis in the smectic-*A* (Sm*A*) phase and this rotation is partially frozen out in the Sm*C* phase [1]. If McMillan's idea is correct, the Sm*C** phase ought to have a spontaneous polarization $P_s$ along the local $C_2$ axis. In 1975, Meyer *et al.* realized this and proved it experimentally in the Sm*C** phase of DOBAMBC [2,3]. Since then, as is well known, various ferroelectric liquid crystalline materials have been synthesized and the physical properties of the ferroelectric liquid crystals (FLCs) have been investigated.

One of the most important findings in FLCs is the sign inversion phenomenon of $P_s$ by the temperature change. In the past, the sign of $P_s$ had been thought as the characteristic of the materials by nature. In 1986, however, two groups independently reported a new class of ferroelectric liquid crystals showing $P_s$ sign inversion [4–6]. Since then, the $P_s$ sign inversion phenomenon has been observed in various systems: single-component substances [4,6,7], two-component mixtures [8–10], and polymer systems [11].

Recently, we performed a detailed texture observation in a single-component material FLC-117 (Chisso) near the $P_s$ inversion temperature $T_{inv}$ and found that $T_{inv}$ depends on the applied voltage. Although the same kind of phenomenon was suggested to occur by Glass *et al.* in the measurement of the pyroelectricity for the ferroelectric liquid crystal S-2-metylbutyl-4-*n*-decanoyloxybiphenyl-4′-carboxylate [12], they did not mention it clearly, so that this is essentially the first report of the phenomenon. Moreover, little is known about the texture near $T_{inv}$. The aim of this paper is to show this experimental result unambiguously and to interpret this phenomenon using a microscopic model.

In the past, the $P_s$ inversion phenomenon has been interpreted by various microscopic models [5,13,14]. Among them, one of the most well-known models is the dipolar-quadrupolar coupling model [14–17]. Based on Landau's theory for the Sm*A*-Sm*C** phase transition, the first mathematical treatment of this model was given by Žekš *et al.* in 1988 [18]. In 1993, Meister and Stegemeyer extended this model to treat $P_s$ sign inversion [14]; they assumed the sign inversion occurs due to the competition between the polar and the quadrupolar orders for the single-particle rotational potential about the molecular long axis. In this paper, we introduce a coupling term between a molecular dipole moment and the magnitude of an applied electric field to the rotational potential and simulate the $P_s$ sign inversion phenomenon under the electric field.

The paper is organized as follows. In Sec. II we will show the experimental results. In Sec. III, to compare with the experimental results, we will define the rotational potential under an electric field, and calculate the numerical solution.

## II. EXPERIMENT

FLC-117, which is known to show the $P_s$ sign inversion, was used in this study [7]. Figure 1 shows the chemical structure and the phase sequence of this single-component material. The glass substrates with patterned indium tin oxide electrodes were washed by acetone, spin coated with polyimide, and rubbed unidirectionally. The two substrates were placed together with 2-$\mu$m polyethylenterephthalate sheet spacers. FLC-117 was introduced into the cell by capillary suction in the isotropic phase. By cooling down from

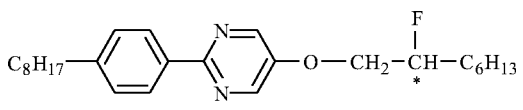


SmC* 47°C SmA 84°C Iso

FIG. 1. The chemical structure and the phase sequence of FLC-117.

*Electronic address: mieda@mbox.op.titech.ac.jp

 

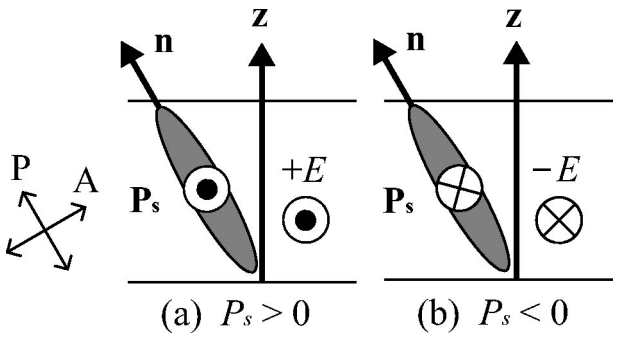


FIG. 2. The sign definition of the $P_s$. The circle with dot and the circle with cross represent the up and down directions with respect to the paper surface, respectively. $E$ represents the magnitude of the electric field. $P$ and $A$ represent the polarizer and analyzer, respectively.

the isotropic phase to the Sm$A$ phase, a single domain with homogeneous alignment was obtained. The Sm$C$* phase was obtained by the cooling process from the Sm$A$ phase. In the Sm$C$* phase under zero electric field, surface stabilized ferroelectric liquid crystal bistable domains [19] were realized, i.e., the uniform textures remain stable after turning off the field (memory effect).

According to convention [20], $P_s$ was defined by

$$\mathbf{P}_s = P_s \frac{\mathbf{z}\times\mathbf{n}}{|\mathbf{z}\times\mathbf{n}|}, \tag{1}$$

where $\mathbf{P}_s$ is the local polarization vector, $\mathbf{z}$ is the layer normal vector, and $\mathbf{n}$ is the director. The definition of the sign of $P_s$ is illustrated in Fig. 2. The magnitude of $P_s$ was determined by the switching-current measurements [21] on applying a rectangular wave voltage (40 V,30 Hz). The sign of $P_s$ was determined by the tilt direction with respect to the layer normal under the dc electric field using a polarizing optical microscope. In Fig. 3, we show the temperature dependence of $P_s$ and magnitude of the tilt angle $\theta$. It is found that the $P_s$ sign inversion occurs between 37 °C and 38.5 °C, which agrees with the previous result [7]. However, since $P_s$ is very

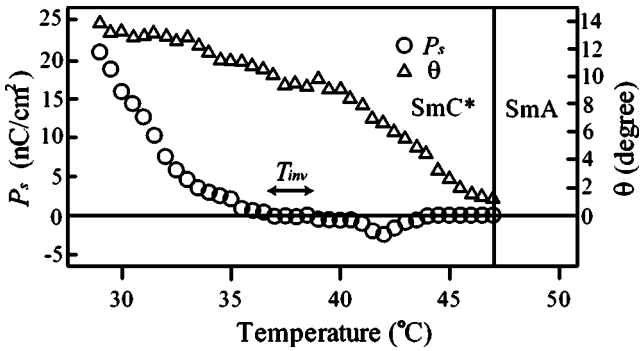


FIG. 3. The temperature dependence of $P_s$ and the magnitude of $\theta$ for FLC-117 in a 2-$\mu$m cell. Circles and triangles represent $P_s$ and $\theta$, respectively. $P_s$ sign inversion occurs between 37 °C and 38.5 °C.

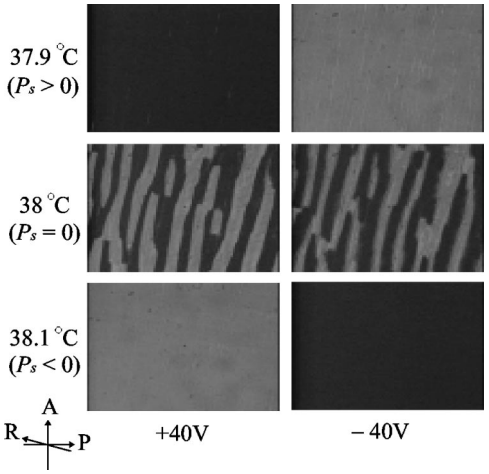


FIG. 4. The microphotographs of a 2-$\mu$m-thick FLC-117 sample cell between crossed polarizers. $P$, $A$, and $R$ represent polarizer, analyzer, and rubbing directions, respectively. At 37.9 °C and at 38.1 °C, $P_s$ signs are positive and negative, respectively. At 38 °C, both dark and bright views coexist, and the bistable domains show no response to the field, indicating that $P_s$ is zero and $T_{inv} = 38$ °C.

small near the inversion point, the precise value of $T_{inv}$ is not easy to be determined only by the switching current measurement.

The $P_s$ inversion process could be directly observed by using a polarizing microscope. Texture observation was made under a rectangular wave of 0.05 Hz with 40 V. The polarizer and analyzer were set to be crossed and arranged to give a dark view for the situation of Figs. 2(a) and 2(b); positive and negative voltages give a dark view for $P_s > 0$ and $P_s < 0$, respectively.

Figure 4 shows microphotographs near $T_{inv}$. At 37.9 °C, $P_s$ is positive, since the situation given by Fig. 2(a) is obtained. At 38.1 °C, on the contrary, the behavior is opposite to that for 37.9 °C; $P_s$ is negative. At 38 °C, both dark and bright views coexist with the tilt angle 9.5°, and the bistable domains do not respond to the field, indicating that $P_s$ is zero. Namely, $T_{inv}$ is 38 °C . In this way, from the direct texture observation, the exact inversion point could be determined.

Moreover, we measured the electro-optic response by applying a triangular wave field near the inversion temperature. The frequency and the amplitude of the applied triangular voltage were 0.1 Hz and 80 V, respectively. At 37 °C, bistable switching was observed, as shown in Fig. 5(a). Bistable switching was also observed at 39 °C, but the phase is opposite to that at 37 °C, as shown in Fig. 5(c). These results indicate that the signs of $P_s$ are opposite at 37 °C and 39 °C. Stars and circles in Fig. 5 specify the response by positive and negative $P_s$, respectively. An interesting electrooptic response was observed at 38 °C [Fig. 5(b)]. At a voltage higher than 40 V, the behavior is the same as that at 37 °C, as marked by stars. Therefore, $P_s$ is positive above 40 V. On the other hand, the response below 40 V shows that $P_s$ is negative.

To investigate the unusual switching in Fig. 5(b), at

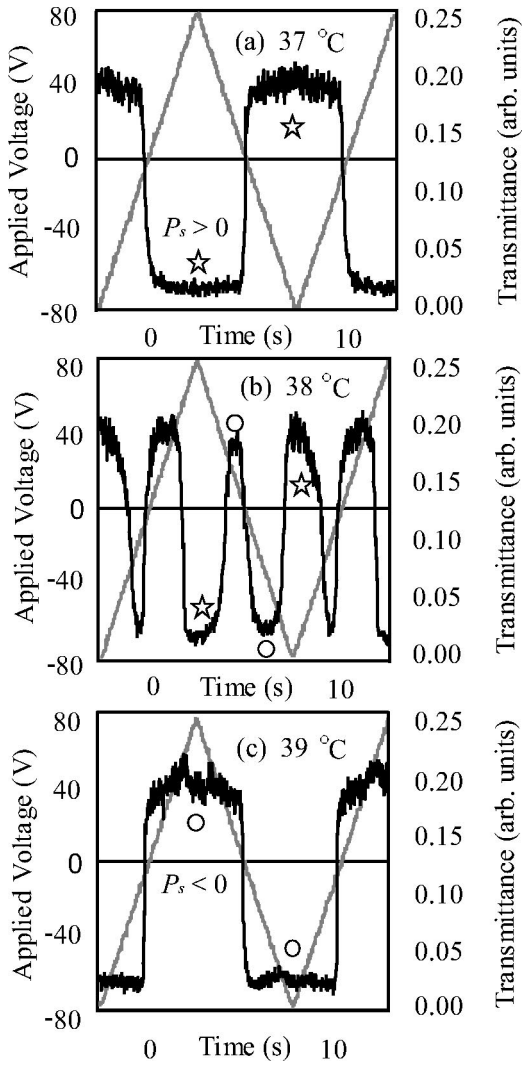


FIG. 5. The optical response for a triangular wave of 0.1 Hz with 80 V at (a) 37 °C, (b) 38 °C, and (c) 39 °C. Stars and circles specify the optical response for $P_s>0$ and $P_s<0$, respectively. At 38 °C, $P_s$ is positive at a high voltage region and negative at a low voltage region.

38 °C we applied a rectangular wave field of 0.05 Hz with different voltages (20 V, 40 V, 80 V) and texture observation was executed. For 40 V, bistable domains show no switching [Fig. 6(b)]. For 20 V, switching is observed, as shown in Fig. 6(a), which indicates that $P_s$ is negative. On the other hand, for 80 V, the switching indicating positive $P_s$ was observed [Fig. 6(c)]. Of course, these results are consistent with the result of the electro-optic response in Fig. 5(b). But these results suggest the possibility that $T_{inv}$ has an applied voltage dependence, $T_{inv} \neq 38$ °C under 20 V and 80 V.

The shift of $T_{inv}$ under 20 V and 80 V was confirmed by the same direct texture observation made under 40 V. The results are given in Table I. This table shows that $T_{inv}$ increases with the increase of the applied voltage strength.

It is important to emphasize that the thermal effect of the voltage does not lead to this behavior. Namely, if higher voltage causes a higher temperature of the cell, the observed $T_{inv}$ should shift toward a lower temperature. This is just

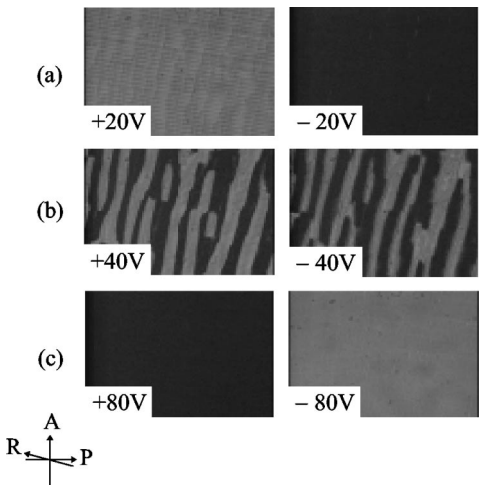


FIG. 6. The applied voltage dependence of the texture at 38 °C. *P*, *A*, and *R* represent polarizer, analyzer and rubbing directions, respectively. The voltage sequence is (a) 20 V, (b) 40 V, and (c) 80 V.

opposite to our experimental results. In this way, we could unambiguously conclude that $T_{inv}$ for FLC-117 has an applied voltage dependence.

## III. DISCUSSION

### A. A molecular model for $P_s$ sign inversion

$P_s$ originates from the hindered rotational motion about the long molecular axis. To describe the model, right-handed rectangular laboratory coordinates $(x,y,z)$ and right-handed rectangular molecular coordinates $(\xi,\eta,\zeta)$ are introduced (Fig. 7), where the $z$ axis is the smectic layer normal, $y$ is the $C_2$ axis, $\zeta$ is the molecular long axis, and $\xi$ is the axis of the electric dipole moment projected on the $\xi$-$\eta$ plane. Moreover, the angles $(\theta,\psi)$ are introduced to describe the relation between $(x,y,z)$ and $(\xi,\eta,\zeta)$, where $\theta$ is the tilt angle from the $z$ axis, and $\psi$ is the rotational angle about the $\zeta$ axis (we define the counterclockwise rotation to be positive). Now we assume that molecular energy is determined by a molecular potential $V_0(\psi)$. The potential under an electric field is given by

$$V(\psi) = V_0(\psi) - \mu_{\text{eff}} E. \tag{2}$$

Here, $E$ and $\mu_{\text{eff}}$ are the magnitudes of the applied electric field and the effective molecular dipole moment for the $y$ direction, respectively. Generally, the molecular distribution function $f(\psi)$ is given by

TABLE I. The applied voltage dependence of the $P_s$ inversion temperature $T_{inv}$ determined by the direct texture observation.

| Applied voltage (V) | $P_s$ inversion temperature (°C) |
|---|---|
| 20 | 37.9 |
| 40 | 38 |
| 80 | 38.1 |

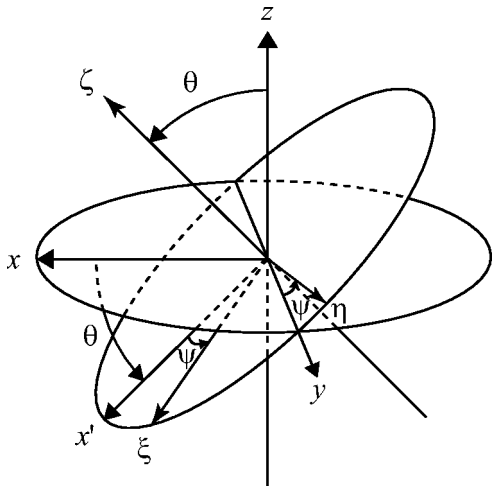


FIG. 7. The definition of laboratory coordinates $(x,y,z)$, molecular coordinates $(\xi,\eta,\zeta)$, and the angles $(\theta,\psi)$. $x'$ axis represents the $\xi$ axis at $\psi=0$.

$$f(\psi)=\frac{1}{Z}\exp\left(\frac{-V(\psi)}{k_BT}\right), \tag{3}$$

where $Z$ is the partition function, $k_B$ is the Boltzmann constant, and $T$ is the temperature. Using this distribution function, $P_s$ is given by

$$P_s=N\langle\mu_{\text{eff}}\rangle=N\mu_\xi\langle\sin\psi\rangle, \tag{4}$$

where $N$ is the number density of the molecule, $\langle\cdots\rangle$ represents the ensemble average, and $\mu_\xi\,(>0)$ is the $\xi$ component of the molecular dipole moment. The sign of $P_s$ is determined by $\langle\sin\psi\rangle$. Here let us consider the mechanism of $P_s$ sign inversion. Suppose that $V_0(\psi)$ has a symmetric form at $\psi=\psi_0\ (>0)$ as shown in Fig. 8(a), namely $V_0(\psi_0-\psi)=V_0(\psi_0+\psi)$; such a symmetric potential was actually adopted as the binding site model in Ref. [22]. However, the sign inversion is impossible in this potential because the population for $\psi>0$ is more than that for $\psi<0$ for all temperatures. On the other hand, if molecular chirality is very strong and $V_0(\psi)$ has the asymmetric form as shown in Fig. 8(b), sign inversion is possible. In this case, because of the asymmetry of the potential, at low temperature, $\psi>0$ has a large population, while at high temperature, $\psi<0$ is more populated.

### B. Numerical calculation using an asymmetric potential

To calculate the numerical solution of the electric field effect on $T_{inv}$, we consider a more realistic potential. In general, the potential should vanish at the Sm*A*-Sm*C** transition point, because the molecules in the Sm*A* phase rotate freely about molecular long axes. To consider this effect, we introduce the $\theta$ dependent potential $V_0(\theta,\psi)$, where $\theta$ is the primary order parameter of the Sm*C** phase. For $\theta$ dependence, we assume the following form:

$$V_0(\theta,\psi)=(\theta+\theta^2+\cdots+\theta^n+\cdots)V_0(\psi), \tag{5}$$

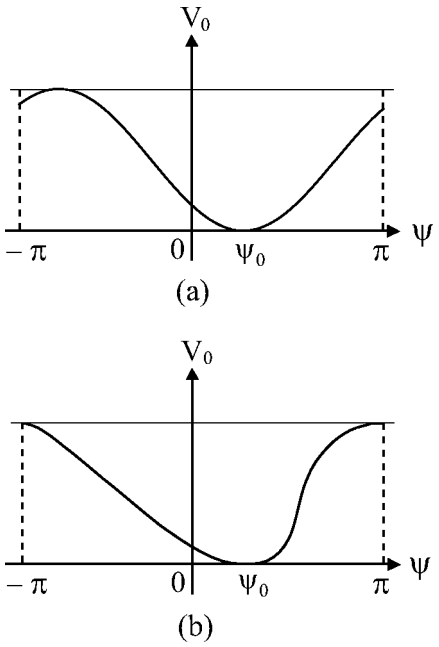


FIG. 8. (a) The symmetric rotational potential function. The $\psi_0$ represents the angle showing the potential minimum. (b) The asymmetric rotational potential function arising from the strong chirality. If the sign of the chirality is inverted, $V_0(\psi)$ is reversed with respect to the $\psi=0$. The $\psi_0$ locates in the positive $\psi$ region in the present experimental condition as in the figure, hence $P_s>0$ at low temperatures.

where the constant term is neglected, since only the relative value is important. Moreover, we expand $V_0(\psi)$ as a Fourier series:

$$V_0(\psi)=D_1\cos(\psi-\omega_1)+D_2\cos 2(\psi-\omega_2)+\cdots+D_n\cos n(\psi-\omega_n)+\cdots, \tag{6}$$

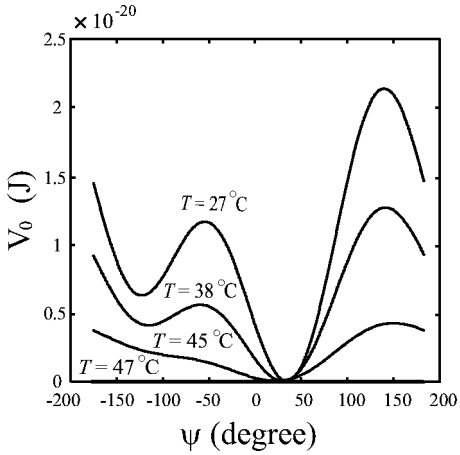


FIG. 9. The temperature dependence of the asymmetric potential function represented by the Fourier expansion. The parameters used for this calculation are $A=4.07\times10^{-22}$, $B=0.3\times10^{-22}$, $\omega_1=-19°$, $\omega_2=40.5°$, and $\theta_0=3.25$. Temperature sequence is 27 °C, 38 °C, 45 °C, and 47 °C.

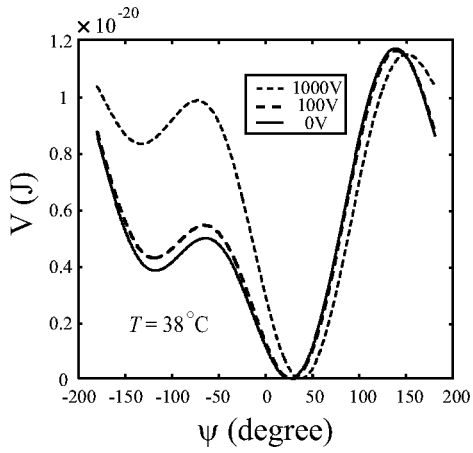


FIG. 10. The applied electric field dependence of the asymmetric rotational potential function. We assumed that the sample was introduced between two electrodes with a 2-$\mu$m gap. The sequence of the applied voltage is 0-V bias=0 V/cm, 100-V bias=5 $\times 10^5$ V/cm, and 1000-V bias=$5\times 10^6$ V/cm. In this calculation, we put $\mu_\xi = 2$ D.

where $D_n$ are the expansion coefficients and $\omega_n$ are the phases. In particular, we use the following potential

$$V_0(\theta,\psi) = -A\theta\cos(\psi-\omega_1) - B\theta^2\cos 2(\psi-\omega_2), \quad (7)$$

where $A>0$ and $B>0$, which has been proposed by Žekš *et al.* [18]. This equation is the most simple potential satisfying the symmetry requirement $V_0(\theta,\psi)=V_0(-\theta,\psi+\pi)$. According to the Landau theory, the temperature dependence of $\theta$ is given by

$$\theta = \theta_0(T_c - T)^{0.5}, \quad (8)$$

where $\theta_0$ is the proportional constant and $T_c$ is the Curie temperature for the Sm*A*-Sm*C** phase transition. Figure 9 shows the temperature dependence of $V_0(\psi)$. Above $T_c = 47$ °C, since the molecules rotate freely, the rotational potential vanishes. Under the electric field, the potential is given by Eq. (2). Figure 10 shows the electric field dependence of the potential function. It is found that the stronger the magnitude of the electric field is, the bigger the potential deviation is. Moreover, the molecular dipole moment under an electric field is obtained by using Eq. (4). Figure 11 shows the temperature and the applied electric field dependence of the average effective dipole moment. It is clearly found that $P_s$ inversion has occurred. From this figure, it is also found that $T_{inv}$ has the applied voltage dependence. Namely, when the applied voltage increases, $T_{inv}$ also increases, being consistent with the present experiment.

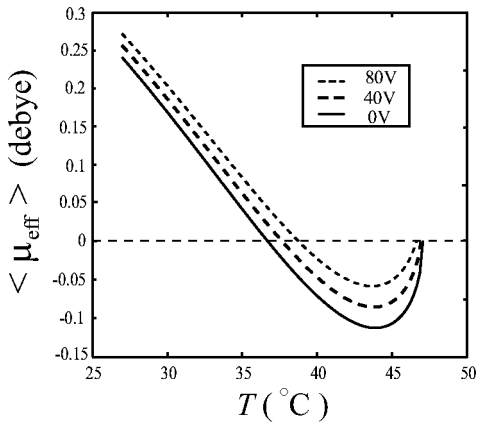


FIG. 11. The temperature and the applied electric field dependence of the average effective dipole moment. The sequence of the applied voltage is 0-V bias=0 V/cm, 40-V bias=$20\times 10^4$ V/cm, and 80-V bias=$40\times 10^4$ V/cm.

## IV. CONCLUSION

Under the electric fields, the ferroelectric liquid crystal FLC-117, which exhibits the $P_s$ sign inversion phenomenon, was studied. From the analysis of the electro-optic response and the direct texture observations by using a polarizing microscope, it was confirmed that the inversion temperature $T_{inv}$ of $P_s$ increases with the increase of the applied voltage strength. To explain this applied voltage dependence of $T_{inv}$, we introduced a coupling term between a molecular dipole moment and the magnitude of an electric field applied to the asymmetric rotational potential about the molecular long axis. The numerical calculations using this potential were in accordance with our experimental results.

## ACKNOWLEDGMENTS

The authors thank Chisso Co. for the supply of a good quality sample. This work is partly supported by a Grant-in-Aid for Scientific Research on Priority Area (B) (12129202) by the Ministry of Education, Science, Sports and Culture.

[1] W.L. McMillan, Phys. Rev. A **8**, 1921 (1973).
[2] R.B. Meyer, L. Liebert, L. Strzelecki, and P. Keller, J. Phys. (Paris) **36**, L69 (1975).
[3] R.B. Meyer, Mol. Cryst. Liq. Cryst. **40**, 33 (1977).
[4] J. W. Goodby, E. Chin, T. M. Leslie, J. M. Geary, and J. S. Patel, in Abstracts of the 11th International Liquid Crystal Conference, Berkeley, 1986 (unpublished).
[5] J.S. Patel and J.W. Goodby, Philos. Mag. Lett. **55**, 283 (1987).
[6] N. Mikami, R. Higuchi, T. Sakurai, M. Ozaki, and K. Yoshino, Jpn. J. Appl. Phys., Part 2 **25**, L833 (1986).
[7] S. Saito, K. Murashiro, M. Kikuchi, D. Demus, T. Inukai, M. Neundorf, and S. Diele, Ferroelectrics **147**, 367 (1993).
[8] Y. Fuwa, K. Myojin, H. Moritake, M. Ozaki, K. Yoshino, T. Tani, and K. Fujisawa, Jpn. J. Appl. Phys., Part 1 **33**, 5488 (1994).
[9] H. Stegemeyer, A. Sprick, M.A. Osipov, V. Vill, and H.-W. Tunger, Phys. Rev. E **51**, 5721 (1995).
[10] M. Ozaki, Y. Fuwa, K. Nakayama, K. Yoshino, T. Tani, and K. Fujisawa, Ferroelectrics **214**, 51 (1998).
[11] G. Scherowsky, B. Brauer, K. Grünegerg, U. Müller, L. Komi-

tov, S.T. Lagerwall, K. Skarp, and B. Stebler, Mol. Cryst. Liq. Cryst. Sci. Technol., Sect. A **215**, 257 (1992).
[12] A.M. Glass, J.W. Goodby, D.H. Olson, and J.S. Patel, Phys. Rev. A **38**, 1673 (1988).
[13] D.J. Photinos and E.T. Samulski, Science **270**, 783 (1995).
[14] R. Meister and H. Stegemeyer, Ber. Bunsenges. Phys. Chem. **97**, 1242 (1993).
[15] B. Urbanc and B. Žekš, Liq. Cryst. **18**, 483 (1995).
[16] Z. Raszewski, J. Kędzierski, P. Perkowski, J. Rutkowska, W. Piecek, J. Zieliński, J. Żmija, and R. Dąbrowski, Mol. Cryst. Liq. Cryst. Sci. Technol., Sect. A **328**, 255 (1999).
[17] Z. Raszewski, P. Perkowski, J. Kędzierski, J. Rutkowska, W. Piecek, J. Zieliński, J. Żmija, R. Dąbrowski, and R.N.V.R. Reddy, Proc. SPIE **4147**, 62 (2000).
[18] B. Žekš, T. Carlsson, C. Filipič, and B. Urbanc, Ferroelectrics **84**, 3 (1988).
[19] N.A. Clark and S.T. Lagerwall, Appl. Phys. Lett. **36**, 899 (1980).
[20] S.T. Lagerwall and I. Dahl, Mol. Cryst. Liq. Cryst. **114**, 151 (1984).
[21] Ph. Martinot-Lagarde, J. Phys. (Paris) **38**, L17 (1977).
[22] D.M. Walba, S.C. Slater, W.N. Thurmes, N.A. Clark, M.A. Handschy, and F. Supon, J. Am. Chem. Soc. **108**, 5210 (1986).